



Ministry of Science, Research & Technology
Iranian Research Organization
for Science and Technology

A modified Marmottant model to study the effects of a shell rupture on the subharmonic threshold of encapsulated microbubbles

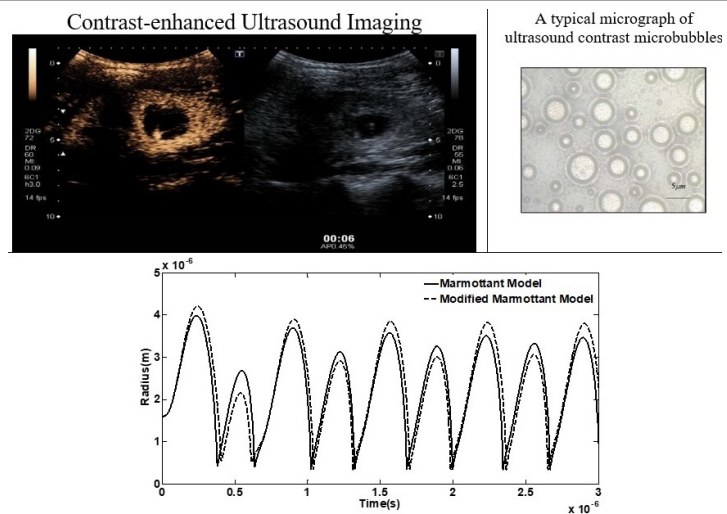
Miralam Mahdi*, Saber Khalili, Majid Rahimi

Faculty of Mechanical Engineering, Shahid Rajaee Teacher Training University, Tehran, Iran

HIGHLIGHTS

- A modified model for the Marmottant model was investigated.
- κ^S in this model gradually decreases after rupturing the shell until it becomes zero.
- The model offers a lower subharmonic threshold than the Marmottant model.

GRAPHICAL ABSTRACT



ARTICLE INFO

Article history:

Received 27 June 2021
Revised 08 March 2022
Accepted 13 April 2022

Keywords:

Encapsulated microbubble
Subharmonic threshold
Dilatational interfacial viscosity

ABSTRACT

This study considers the radial behavior of a coated microbubble after a shell rupture using the Marmottant model. The surface tension of the encapsulated microbubble should equal the free bubble in the rupture state of the Marmottant model. Despite the assumption that the bubble is considered free in the third state, dilatational interfacial viscosity is constant in the equation in this model. This paper assumes that dilatational interfacial viscosity decreases gradually after shell rupture until it becomes zero. The decrease of dilatational interfacial viscosity caused by the shell rupture significantly affects radial behavior and the nonlinear response of the encapsulated microbubble, such as subharmonic response. Because the subharmonic response is extensively used in ultrasound imaging, the effect of a decrease in dilatational interfacial viscosity on the subharmonic threshold needs to be investigated. In figures showing the radius versus time and the frequency response of the coated microbubble, it is observed that at high excitation pressure, the proposed model is more nonlinear than the Marmottant model, resulting in a lower subharmonic threshold.

* Corresponding author: Tel.: +9821-22970052 ; Fax: +9821-22970052 ; E-mail address: m.mahdi@sru.ac.ir

DOI: 10.22104/JPST.2022.5027.1186

1. Introduction

Encapsulated microbubbles are used extensively in ultrasound imaging and therapy. The role of these microbubbles is to scatter and reflect transmitted Ultrasound from the targeted spot due to the difference in acoustic impedance. Unlike tissue, blood is a poor reflector of Ultrasound. Micron-sized microbubble contrast agents injected intravenously into the blood flow are used to improve these properties. Microbubble contrast agents (1 to 10 μm) are stabilized with a shell (e.g., lipid or albumin). These microbubbles are used in ultrasound imaging of different body organs and the cardiovascular system. Adding a shell to the microbubble prevents fast dissolution and increases its stability. The shell changes surface tension and subsequently affects the microbubble's radius behavior and frequency response. Therefore, a precise understanding of the dynamic behavior of the coated microbubble is a critical topic considered by many researchers in the last years.

The Rayleigh-Plesset (RP) equation describes the radial behavior of a free bubble in an infinite fluid in which the pressure changes frequently, but this equation changes by adding a shell. Researchers have carried out many different studies on the RP equation over the past two decades. De Jong *et al.* investigated the influence of the bubble shell on the radial behavior of a bubble and defined two parameters, shell elastic (S_p) and viscous shell friction (S_v) [1]. Church created a theoretical model for the radial behavior of an encapsulated microbubble by considering a nanometer-thick shell and an incompressible rubbery material as the microbubble [2]. In this study, a coated microbubble was assumed in a Newtonian fluid, and results showed that the resonant frequency of the coated microbubble rose after adding a shell, increasing the rigidity of the microbubble [3,4]. Hoff *et al.* proposed a new model for the radial behavior of an encapsulated microbubble with a thin shell [5]. This work analyzed oscillations of the microbubble to predict acoustic scattering and attenuation from the microbubble. Chatterjee *et al.* proposed the simplest interfacial rheological model (Newtonian model) for the shell of the encapsulated microbubble [6]. Shankar *et al.* showed that reducing the actual damping reduces the threshold pressure for subharmonic initiation [7]. Finally, Sarkar *et al.* developed a viscoelastic interface model for a thin-shelled encapsulated microbubble and investigated the scattered responses of a solution of the

encapsulated microbubble (Sonazoid) [8].

Marmottant *et al.* proposed a model that simulates an encapsulated microbubble's nonlinear behavior at high excitation pressure [9]. This model predicts the buckling and rupture of a coated bubble, considering the bubble's surface tension at three different states. Emmer *et al.* investigated the onset of an encapsulated microbubble oscillation [10]. They concluded that the behavior of the microbubble is nonlinear, and the oscillation is asymmetric at high excitation pressure, which means the compression of the bubble is different from its expansion. De Jong *et al.* studied the highly nonlinear behavior of an encapsulated microbubble using the Marmottant model [11]. Results showed that the compression-only behavior appears at high excitation pressure, which means the compression phase of a coated microbubble is greater than the expansion phase. Tu *et al.* analyzed the radial behavior of an encapsulated microbubble [12] (SonoVue employing three types of modified RP equations and estimated the shell elasticity and viscosity of SonoVue microbubbles for different radiuses. Their results showed that the linear oscillation was similar in all the models. Dinokov *et al.* fitted an equation for these data [13].

Paul *et al.* proposed a new model for the nonlinear behavior of a bubble to predict the fundamental and subharmonic responses of an encapsulated microbubble (Sonazoid). Moreover, they studied the frequency response of the microbubble contrast agents [14,15]. Overvelde *et al.* studied the dynamic behavior of an encapsulated microbubble experimentally and numerically [16]. They investigated the effect of excitation pressure on the resonance frequency of an encapsulated microbubble. They also studied the effect of excitation frequency on thresholding behavior. Helfield *et al.* conducted an experimental observation of the influences of fluid viscosity on the radial behavior of an encapsulated microbubble, and they perceived that an increase in the liquid viscosity restricts the amplitude of the oscillations [17]. Furthermore, the subharmonic response from encapsulated microbubbles depends on the ambient pressure variation, and this dependence has been used in noninvasive local organ-level pressure estimation.

One of the most important reasons to study the radial behavior of the encapsulated microbubble is to investigate the frequency response of the microbubble in the ultrasound field. These microbubbles generate subharmonic frequency components under certain

excitations conditions used for subharmonic imaging. Forsberg *et al.* investigated the subharmonic response of the contrast agents Optison and Levovist [18,19]. They observed that the subharmonic response depends significantly on excitation and hydrostatic pressure amplitudes. Shankar *et al.* examined the advantages of the subharmonic response of microbubble contrast agents [20]. To better understand ultrasound contrast agents (UCA's) behavior, Adam *et al.* studied the effects of ambient pressure on the acoustic scattering of Optison in three different modes [21]. Andersen and Jensen presented an approach for investigating the ambient pressure sensitivity of a contrast agent using diagnostic ultrasound [22]. They experimentally examined the subharmonic response from a microbubble contrast agent as a function of ambient overpressure. Sarkar *et al.* investigated the effects of pressure and frequency on the subharmonic response and found they reach a critical frequency ratio with maximum subharmonic response [23]. Forsberg *et al.* achieved an excellent correlation between the amplitude of the subharmonic component and the hydrostatic pressure at the growth stage of subharmonic production [24]. Other similar studies have been carried out [25-27].

Since the encapsulated microbubbles are destroyed above a critical excitation level, further studies are required to determine the subharmonic threshold for encapsulated microbubbles. Therefore, specifying the excitation threshold of the subharmonic frequency is crucial for nondestructive subharmonic applications. Chatterjee *et al.* examined the destruction of the encapsulated microbubbles (Definity) under acoustic excitation [27]. Katiyar *et al.* performed a numerical study of several models for encapsulated microbubbles to determine the excitation threshold for the subharmonic generation [28,29]. Different studies have been conducted for this purpose [30,31].

The viscosity parameter is considered constant in shell models. Moreover, its effect is not considered after the rupture of the shell. Most models deal with the surface tension effect for modeling, but viscosity also affects the resonance frequency and subharmonic threshold. In this paper, the effects of shell rupture on the nonlinear behavior of the microbubble contrast agent Sonazoid are investigated. In Sec. II, a modified PR equation is defined to decrease the dilatational interfacial viscosity after rupturing the shell in the Marmottant model. Also, the Exponential elasticity model, Marmottant model,

and Modified Marmottant model are discussed in further detail. Lastly, the numerical studies are validated. In Sec. III, the radial behavior of an encapsulated microbubble (Sonazoid) is briefly studied using the Marmottant and modified Marmottant models. Then, a numerical investigation of these models is executed to determine the excitation threshold for a subharmonic generation as a function of frequency. Finally, we show how a decrease in the dilatational interfacial viscosity leads to different variations of the subharmonic threshold with normalized excitation frequency. Section 4 presents the study's conclusion.

2. Encapsulated bubble dynamics

If a liquid containing a microbubble is exposed to an ultrasound field in which ambient pressure changes frequently and the amplitude of excitation pressure is significant enough, the microbubble starts to oscillate. In the simplest case, the microbubble is spherical during pressure fluctuations. Microbubble oscillations cause radial changes that mathematical equations can simulate. Most models defined for encapsulated microbubbles are based on a modified RP equation. Added terms represent the contributions caused by viscoelastic stresses produced in the encapsulation. In these models, viscoelastic terms can be added as $\gamma(R)$ and $\kappa^S(R)$, the efficient surface tension and efficient dilatational viscosity, respectively, as shown in Eq. (1).

$$\rho \left(R\ddot{R} + \frac{3}{2}\dot{R}^2 \right) = P_{G0} \left(\frac{R_0}{R} \right)^{3k} \left(1 - \frac{3k\dot{R}}{c} \right) - \frac{2\gamma(R)}{R} - \frac{4\dot{R}}{R^2} \kappa^S(R, \dot{R}) - 4\mu \frac{\dot{R}}{R} - P_0 + p_A(t) \quad (1)$$

where P_0 is the hydrostatic pressure, c is the speed of sound, and $p_A(t)$ is the excitation pressure (considered sinusoidal in our investigations). Also, initial conditions are $(t = 0) = R_0$, and $\dot{R}(t = 0) = 0$.

2.1. Exponential elasticity model (EEM) [15]

This model expresses the progressive decrease of elasticity using an exponential decline, which is defined by Eq. (2).

$$E_s = E_0^s \beta \exp(-\alpha^s \beta) \quad (2)$$

In this equation, α^s and E_0^s are specified (Table 1),

$\beta = (R^2 - R_E^2) / R_E^2$ is the variation of area fraction, and R_E is the equilibrium radius with zero elastic stress. The efficient surface tension and efficient dilatational viscosity are defined as Eq. (3).

$$\gamma(R) = \gamma_0 + E_s \beta, \quad \kappa^S(R) = \kappa^S(\text{constant}) \quad (3)$$

$$R_E = R_0 \left[1 + \left(\frac{1 - \sqrt{1 + 4\gamma_0 \alpha^S / E_0^S}}{2\alpha} \right) \right]^{-1/2}$$

where γ_0 is the constant tension in the un-deformed state.

Characterization parameters (γ_0 , κ^S , E_0^S , ...) were determined by Paul *et al.* using attenuation [15]. They then used the attenuation measurements through a Sonazoid solution to find the characteristic parameters relating to this model [8]. To determine the characteristic parameters related to each model, they used an error function between the measured and model attenuation. Therefore, the parameters were obtained using the minimized error function in MATLAB. Table 1 shows the property values for the Sonazoid microbubble used in this study.

2.2. Marmottant model [9]

At high excitation pressure, Marmottant *et al.* provided a model that considers three different states for the surface tension [9]: the buckling state in which the surface tension of a coated bubble is supposed to be zero ($R \leq R_{buckling}$), the elastic state ($\gamma(R) = \chi (A/A_{buckling} - 1)$), and the rupture state where the bubble is considered to be free (without shell); in this state, the radius of the bubble is larger than $R_{rupture}$ ($R_{rupture} = R_{buckling} (1 + \sigma_{water} / \chi)^{1/2}$). The efficient surface tension and dilatational interfacial viscosity are considered as Eq. (4).

$$\gamma(R) = \begin{cases} 0 & \text{for } R \leq R_{buckling} \\ \chi \left(\frac{R^2}{R_{buckling}^2} - 1 \right) & \text{for } R_{buckling} \leq R \leq R_{rupture} \\ & \text{and } \kappa^S(R) = \kappa^S(\text{constant}) \\ \sigma_w & \text{if ruptured and for } R \geq R_{rupture} \end{cases} \quad (4)$$

In this equation, it is supposed that $R_{buckling} = R_0$, hence the bubble surface tension is zero in the initial state ($\sigma(R_0) = 0$), and the pressure is in equilibrium on the bubble surface. The modified RP equation for this model is defined as Eq. (5).

$$\rho \left(R\ddot{R} + \frac{3}{2}\dot{R}^2 \right) = \left[P_0 + \frac{2\gamma(R_0)}{R_0} \right] \left(\frac{R_0}{R} \right)^{3\gamma} \left(1 - \frac{3\gamma\dot{R}}{c} \right) \\ , - \frac{2\gamma(R)}{R} - \frac{4\dot{R}}{R^2} \kappa^S - 4\mu \frac{\dot{R}}{R} - P_0 + P_A(t) \quad (5)$$

2.3. Modified Marmottant model

Among the proposed models for the nonlinear behavior of an encapsulated microbubble, the Marmottant model has the advantage of being closer to experimental results at high excitation pressures than earlier models. This conformity is due to considering the surface tension in three different states, which change with the radius mentioned above. In the Marmottant and other similar models, such as the EEM model [15], the viscosity of the shell (κ^S) is constant unlike, the surface tension that changes with the radius. In the third state (after rupturing of the shell) in the Marmottant model, the surface tension of the coated bubble relaxes equal to the free bubble (σ_w), but the dilatational viscosity is constant. Whereas the bubble is considered free, the dilatational viscosity of the ruptured bubble should not be equal to the previous state ($\kappa^S = \text{constant}$).

In this paper, the Marmottant model is modified, thereby changing the radius; the subsequent subharmonic response from the encapsulated microbubbles is then studied. Unlike the Marmottant model, the dilatational viscosity is not constant after the shell is ruptured but instead decreases gradually. With an increasing area fraction, the gradual decrease of viscosity would be better modeled by an exponential decline. Hence, an equation is defined as a viscosity change after the shell is ruptured and imposed on the Marmottant model. In the EEM model, the elasticity of the shell decreases exponentially as the bubble's surface increases. In this

Table 1. Property values of encapsulated Sonazoid in the Marmottant and exponential models [15].

Marmottant model			Exponential model		
$\kappa^S (\times 10^{-8} \text{ kg.s}^{-1})$	$\chi (\text{N.m}^{-1})$	$R_{buckling}$	$\kappa^S (\times 10^{-8} \text{ kg.s}^{-1})$	$E_0^S (\text{N.m}^{-1})$	α
1.2 (± 0.4)	0.53 (± 0.1)	R_0	1.2 (± 0.4)	0.55 (± 0.1)	1.5 (± 0.05)

study, a similar viscosity change equation is defined for the decreasing dilatational interfacial viscosity (Eq. (6)).

$$\kappa^S = \kappa^S \beta \exp(-\alpha^S \beta) \quad (6)$$

According to the results obtained by Paul *et al.* (Table 1), the value of the shell compressibility χ and the surface dilatational viscosity κ^S for the Marmottant model are the same as the dilatational surface elasticity E_0^S and viscosity κ^S for the exponential elasticity model (EEM) [15]. Since the predicted characterization of the encapsulation is the same for two models (Marmottant and EEM), in this study (in the modified Marmottant model), it is assumed that the amount of κ^S , β , R_E , α^S are equal to the values of the EEM model [15] (Table 1). The dilatational interfacial viscosity changes (κ^S) with the fractional change in the area (β) are shown in Fig. 1.

Fig. 1 shows the area's dilatational interfacial viscosity changes versus fractional change. According to Fig. 1, the initial dilatational interfacial viscosity is a defined number ($\kappa^S = 1.2 \times 10^{-8}$ kg.s⁻¹). In the Marmottant model, this parameter is constant during radial oscillations (even after the rupture of the shell); however, it changes gradually in this study. Here, the dilatational interfacial viscosity decreases when the bubble's radius becomes more than the rupture radius. Eventually, the dilatational interfacial viscosity reaches zero when the shell of the bubble is completely ruptured.

2.4. Validation of numerical model

Our numerical studies were validated with Paul *et al.*'s observations to ensure the accuracy of the results [15]. The radial behavior of the encapsulated microbubble (Fig. 2) was simulated using Eq. (5) and the Marmottant

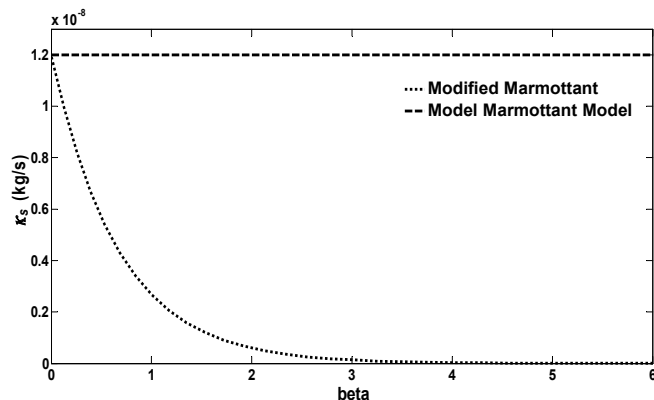


Fig. 1. Amount of dilatational interfacial viscosity versus fractional change in the area.

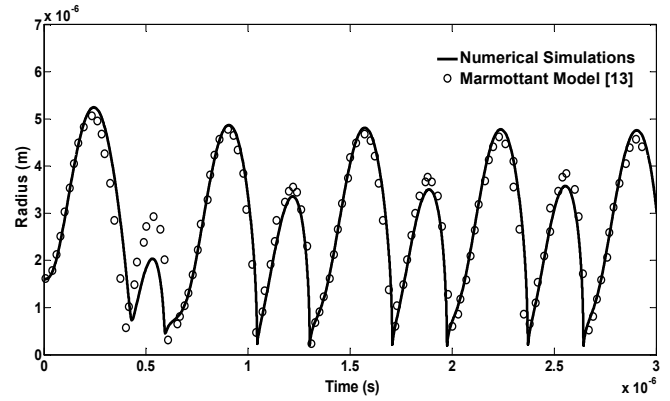


Fig. 2. Validation of numerical investigation using the Marmottant model and Paul *et al.* [15] observations for radial behavior of an encapsulated microbubble ($p_a = 1.5$ MPa, $f = 3$ MHz). The shell parameters of an encapsulated microbubble are ($\chi = 0.53$ N.m⁻¹, $\kappa^S = 1.2 \times 10^{-8}$ kg.s⁻¹).

model. Hence, a sinusoidal excitation pressure with a constant pressure amplitude was imposed on the microbubble contrast agent (Sonazoid). We used $\mu = 0.001$ kg.ms⁻¹, $\rho = 1000$ kg.m⁻³, and $c = 1485$ m.s⁻¹. Additionally, the modified Marmottant model proposed in this study was compared with the Marmottant model in section 3.

3. Results and discussion

In this study, the radial behavior and frequency response of ultrasound contrast agents (Sonazoid, see Table 1) are investigated at high excitation pressure. Here, a sinusoidal excitation pressure consisting of 64 cycles and constant pressure amplitude is imposed on a microbubble contrast agent. We use $\rho = 1000$ kg.m⁻³, $\mu = 0.001$ kg.ms⁻¹, and $c = 1485$ m.s⁻¹. First, the Marmottant and proposed modified Marmottant model were used to study the radial behavior of the encapsulated microbubble. Then, the power spectrum was obtained using scattered pressure $P_s(t)$ on a bubble and by imposing the FFT routine in MATLAB. Finally, the subharmonic threshold for the microbubble was investigated for the two models.

3.1. The effect of a decrease in the dilatational interfacial viscosity on the radial behavior of an encapsulated microbubble

This section investigates the radial behavior of a coated microbubble using the defined equation defined in previous sections to decrease the dilatational interfacial

viscosity. Figs. 3 to 5 show the radius changes of the microbubble (Sonazoid) versus time in the Marmottant and modified Marmottant models. The excitation frequency was constant at 3 MHz, and the excitation pressure was increased. It is evident that the deviation of the two models increases as the excitation pressure increases. This deviation refers to the reduction in

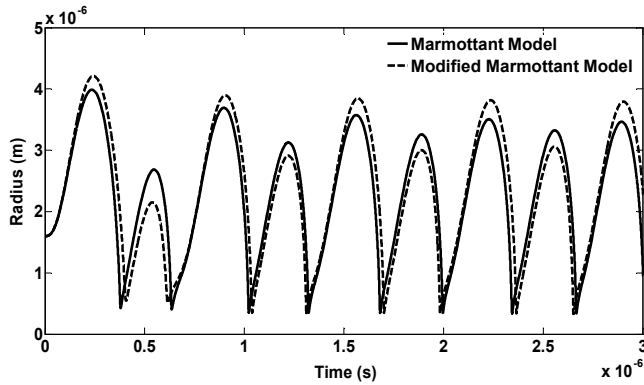


Fig. 3. Radial behavior of encapsulated microbubble (Sonazoid) is predicted in the Marmottant and modified Marmottant models ($p_a = 1 \text{ MPa}, f = 3 \text{ MHz}$).

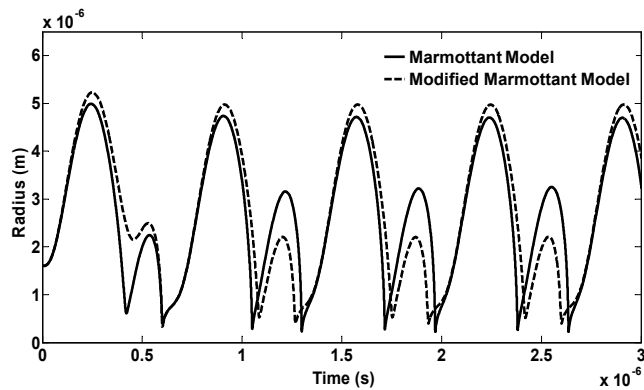


Fig. 4. Radial behavior of encapsulated microbubble (Sonazoid) is predicted in the Marmottant and modified Marmottant models ($p_a = 1.5 \text{ MPa}, f = 3 \text{ MHz}$).

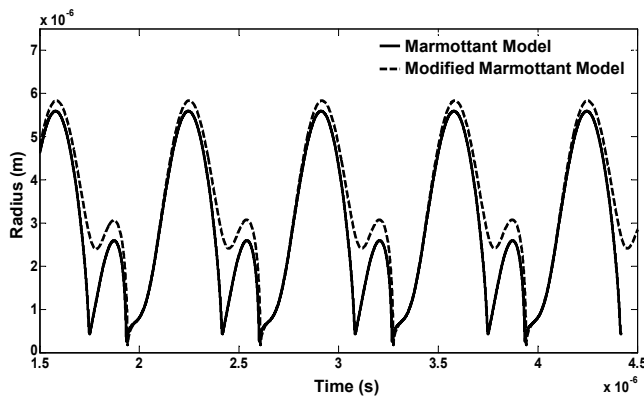


Fig. 5. Radial behavior of encapsulated microbubble (Sonazoid) is predicted in the Marmottant and modified Marmottant models ($p_a = 2 \text{ MPa}, f = 3 \text{ MHz}$).

shell viscosity after the shell ruptures in the modified Marmottant model, increasing the oscillation amplitude. Fig. 6 shows the changes in the microbubble radius versus time in the Marmottant, Modified Marmottant, Constant Elasticity, and Newtonian models. The excitation frequency is 3MHz, and the excitation pressure is 1 MPa.

We also investigated the radial behavior of the microbubble at other frequencies. It was observed that increasing the excitation frequency (from 3 MHz to 6 MHz) decreased the mechanical index (MI) and nonlinearity. Additionally, a lower mechanical index (linear oscillations) postpones the shell rupturing, thereby decreasing the deviation between the two models (Marmottant and modified Marmottant model). Comparing numerical results showed that a decrease in the dilatational interfacial viscosity plays a critical role in the radial behavior of encapsulated microbubbles, specifically at high excitation pressure or a high mechanical index (MI). It was observed that the deviation of the two models at the same excitation pressure at 3 MHz was more than 6 MHz; however, the two models were the same at lower excitation pressures at this frequency (6 MHz). Finally, it can be stated that by adding an equation in the Marmottant model for the decrease of the dilatational interfacial viscosity, this model predicts more nonlinear behavior for the encapsulated microbubble.

3.2. The effect of a decrease in the dilatational interfacial viscosity on the subharmonic threshold

The Eq. (5) for the radial behavior of the encapsulated microbubble is solved using a stiff solver (ODE15s) in

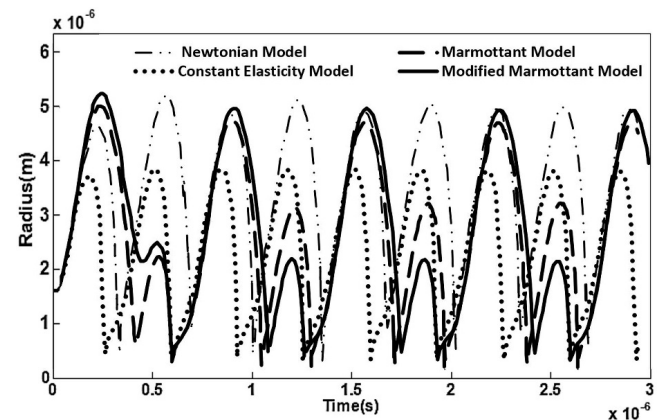


Fig. 6. The radial behavior of the enclosed microbubble (Sonazoid) predicted in the Marmottant model, modified Marmottant model, constant elasticity model, and Newtonian model ($p_a = 1 \text{ MPa}, f = 3 \text{ MHz}$).

MATLAB with initial conditions $R = R_0$ and $\dot{R} = 0$. The scattered acoustic pressure $P_s(t)$ of an encapsulated microbubble is computed as Eq. (7).

$$p_s(r, t) = \rho \frac{R}{r} (2\dot{R}^2 + R\ddot{R}) \quad (7)$$

First, the scattered pressure of the microbubble is calculated. Then because this scattered pressure is in the time domain, the Fast Fourier Transform (FFT) routine of MATLAB is applied to obtain the power spectrum in the frequency domain. The purpose of obtaining the frequency domain is to observe the frequency components, specifically the subharmonic component of the microbubbles. In this section, the variation of the subharmonic component with the excitation pressure is investigated to determine the subharmonic generation threshold. When the excitation pressure rises above a specific value, a distinct subharmonic peak emerges, and this pressure was chosen as the subharmonic threshold. As mentioned above, a rupture of the shell significantly affects the radial behavior and, consequently, the subharmonic response of the microbubble contrast agents. Figs. 7 and 8 show the spectrum of the scattered signals from Sonazoid microbubbles without size distribution and the same radius ($R_0 = 1.6 \mu\text{m}$) as predicted by the Marmottant and modified Marmottant model. The excitation frequency is the same for the two models ($f = 3 \text{ MHz}$), but the excitation pressure is different. It is evident that the subharmonic amplitude is roughly the same in the two models, but the excitation pressure in the modified Marmottant model is lower than in the Marmottant model. This lower subharmonic threshold refers to a decrease in the dilatational interfacial viscosity in the proposed model in this study. In other words, a decrease

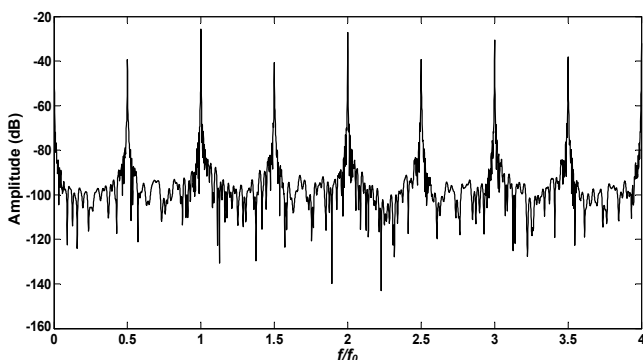


Fig. 7. The spectrum of the scattered signals from Sonazoid microbubbles without size distribution and the same radius ($R_0 = 1.6 \mu\text{m}$) predicted by the Marmottant model at ($f = 3 \text{ MHz}$, $P = 1.5 \text{ MPa}$).

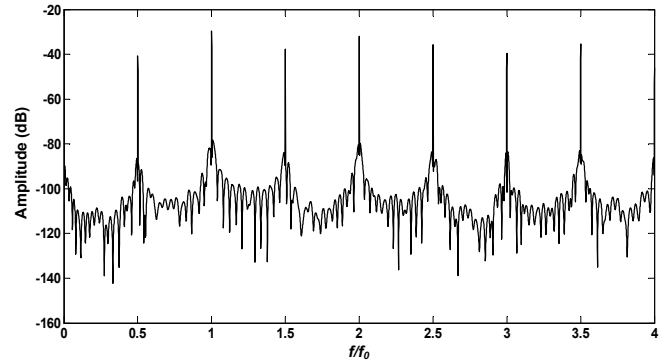


Fig. 8. The spectrum of the scattered signals from Sonazoid microbubbles without size distribution and the same radius ($R_0 = 1.6 \mu\text{m}$) predicted by the Marmottant model at ($f = 3 \text{ MHz}$, $P = 1.15 \text{ MPa}$).

in shell viscosity affects subharmonic amplitude in the same excitation conditions.

The scattering of Ultrasound from Sonazoid microbubbles (with a constant radius $R_0 = 1.6 \mu\text{m}$ and ignoring size distribution) was studied numerically. Since the number of microbubbles with $R_0 = 1.6 \mu\text{m}$ are dominant in a Sonazoid microbubble solution, we investigated the subharmonic response of contrast microbubbles in this radius. Figs. 9 to 11 show the subharmonic response versus excitation pressure. Sarkar *et al.*'s study state that the subharmonic response consists of three different regimes: initial phase, rapid growth, and saturation phase [23]. Initially, the subharmonic component is minor in the two models, but in the modified Marmottant model, this response appears earlier (at a lower subharmonic threshold amplitude) than in the Marmottant model. This lower threshold amplitude refers to a decrease in the dilatational interfacial viscosity imposed on the Marmottant model. In other words, after rupturing of the shell, a decrease of the dilatational interfacial viscosity in the modified Marmottant model increases the nonlinearity and, consequently, affects the subharmonic response of the microbubbles. The subharmonic amplitude increases quickly in the growth phase, and the quantitative subharmonic amplitude in the modified model is more significant than in the Marmottant model. As the excitation pressure amplitude increases, the subharmonic component reaches a saturated state, and the two models are almost the same. Moreover, the growth phase is postponed at higher frequencies because of a decrease in nonlinearity (low MI).

As mentioned above, the decrease of the dilatational interfacial viscosity at high nonlinear oscillation is significant. Given that the subharmonic response

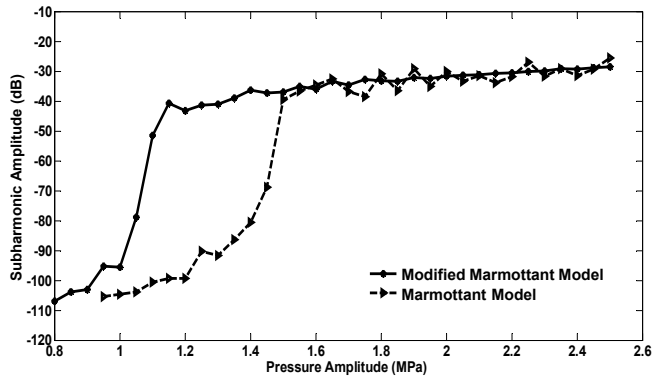


Fig. 9. Scattered subharmonic response of Sonazoid microbubbles without size distribution and the same radius ($R_0 = 1.6 \mu\text{m}$) versus transmitted excitation pressure at ($f = 3 \text{ MHz}$).

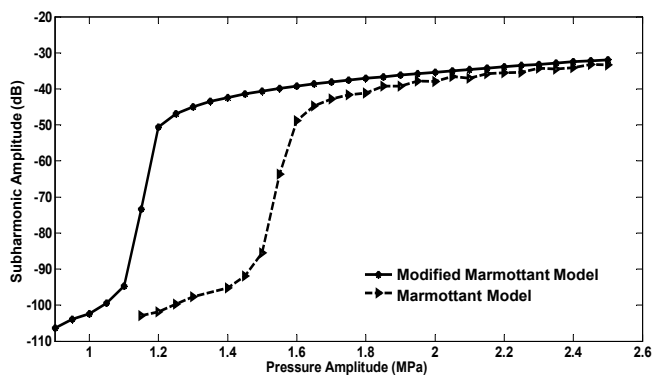


Fig. 10. Scattered subharmonic response of Sonazoid microbubbles without size distribution and the same radius ($R_0 = 1.6 \mu\text{m}$) versus transmitted excitation pressure at ($f = 4.4 \text{ MHz}$).

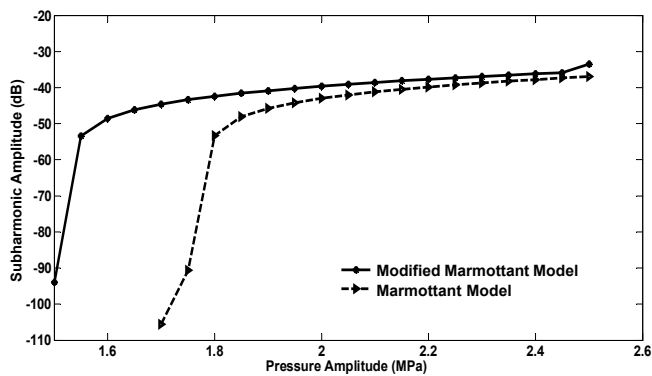


Fig. 11. Scattered subharmonic response of Sonazoid microbubbles without size distribution and the same radius ($R_0 = 1.6 \mu\text{m}$) versus transmitted excitation pressure at ($f = 6 \text{ MHz}$).

appears during the nonlinear oscillation of a bubble, a decrease in the dilatational interfacial viscosity would affect the subharmonic response of the microbubble. So, the effects of decreased dilatational interfacial viscosity on the excitation threshold for subharmonic generation from encapsulated microbubble (Sonazoid) were investigated. Figs. 12 and 13 show the variation of

the subharmonic threshold of a Sonazoid microbubble in the Marmottant and modified Marmottant models at two different radii. It is observed that a decrease in the dilatational interfacial viscosity decreases the subharmonic threshold, especially for microbubbles with small radii. As noted above, the decrease of the dilatational interfacial viscosity is significant as nonlinearity increases. Microbubbles have higher nonlinear behavior than large microbubbles due to the high density of their internal gas, and as a result, the deviation of the two models for small radii bubbles is greater than for large radii bubbles. Also, by increasing the excitation frequency, the mechanical index (MI) and nonlinearity are reduced, which reduces the deviation of the two models because the probability of shell rupture (reduction of shell viscosity) is low. In other words, reducing the shell viscosity in the event of a severe rupture reduces the threshold values, especially at low frequencies. Figs. 12 and 13 show that the deviation between the two models at low frequencies is greater than at high frequencies. In these figures, the excitation

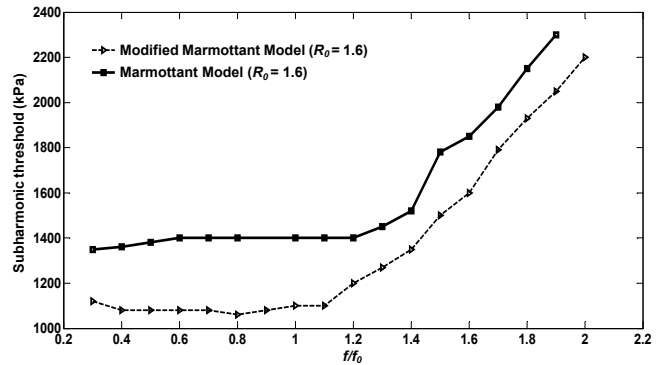


Fig. 12. Variation of the subharmonic threshold of a Sonazoid microbubble with excitation frequency ($R_0 = 1.6 \mu\text{m}$) for the Marmottant and modified Marmottant models.

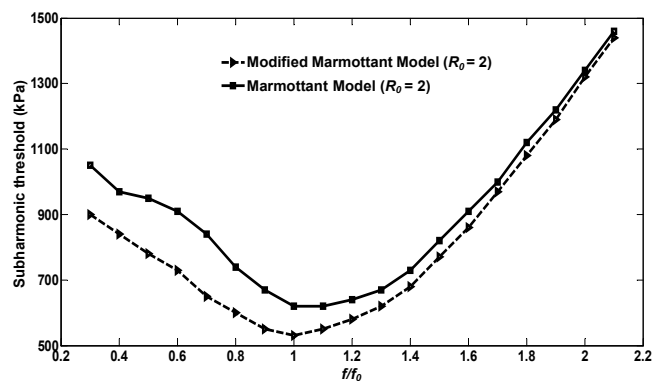


Fig. 13. Variation of the subharmonic threshold of a Sonazoid microbubble with excitation frequency ($R_0 = 2 \mu\text{m}$) for the Marmottant and modified Marmottant models.

frequency is normalized by the resonance frequency of the microbubble. Using Shankar *et al.* and Figs. 12 and 13, it can be concluded that the damping in this model is reduced [7].

4. Conclusions

In this paper, we investigated the decrease of dilatational interfacial viscosity in an encapsulated microbubble at high excitation pressure. We modified the Marmottant model with an equation for the decrease of the dilatational interfacial viscosity imposed on the rupture state. The parameters of this equation are based on the parameters of the EEM model. First, the effect of the decrease of the dilatational interfacial viscosity on the radial behavior of an encapsulated microbubble was investigated by comparing the Marmottant and modified Marmottant models. Results show that at high excitation pressure, where the behavior of the microbubble is nonlinear and the shell ruptures, a decrease in the dilatational interfacial viscosity increases the amplitude of oscillations. However, at low excitation pressure (low level of MI), we found the Marmottant and modified Marmottant models are the same. Therefore, the effect of the decrease of the dilatational interfacial viscosity on the subharmonic threshold of encapsulated microbubbles was studied. The results show that the subharmonic threshold for the modified Marmottant model is lower than the Marmottant model in the same excitation conditions. Furthermore, the deviation of the two models with small radii bubbles is greater than larger bubbles because the tiny microbubbles have more nonlinear behavior than larger ones. Also, by increasing excitation frequency, the deviation of the two models decreases.

References

- [1] N. De Jong, R. Cornet, C.T. Lancee, Higher harmonics of vibrating gas-filled microspheres, Part one: simulations, *Ultrasonics*, 32 (1994) 447-453.
- [2] C.C. Church, The effects of an elastic solid surface layer on the radial pulsations of gas bubbles, *J. Acoust. Soc. Am.* 97 (1995) 1510-1521.
- [3] N. De Jong, L. Hoff, Ultrasound scattering properties of Albnex microspheres, *Ultrasonics* 31 (1993) 175-181.
- [4] S.M. Van der Meer, B. Dollet, M.M. Voormolen, C.T. Chin, A. Bouakaz, N. De Jong, *et al.*, Microbubble spectroscopy of ultrasound contrast agents, *J. Acoust. Soc. Am.* 121 (2007) 648-656.
- [5] L. Hoff, P.C. Sontum, J.M. Hovem, Oscillations of polymeric microbubbles: Effect of the encapsulating shell, *J. Acoust. Soc. Am.* 107 (2000) 2272-2280.
- [6] D. Chatterjee, K. Sarkar, A Newtonian rheological model for the interface of microbubble contrast agents, *Ultrasound Med. Biol.* 29 (2003) 1749-1757.
- [7] P.M. Shankar, P.D. Krishna, V.L. Newhouse, Subharmonic backscattering from ultrasound contrast agents, *J. Acoust. Soc. Am.* 106 (1999) 2104-2110.
- [8] K. Sarkar, W.T. Shi, D. Chatterjee, F. Forsberg, Characterization of ultrasound contrast microbubbles using in vitro experiments and viscous and viscoelastic interface models for encapsulation, *J. Acoust. Soc. Am.* 118 (2005) 539-550.
- [9] P. Marmottant, S. van der Meer, M. Emmer, M. Versluis, N. De Jong, S. Hilgenfeldt, D. Lohse, A model for large amplitude oscillations of coated bubbles accounting for buckling and rupture, *J. Acoust. Soc. Am.* 118 (2005) 3499-3505.
- [10] M. Emmer, A. Van Wamel, D.E. Goertz, N. De Jong, The onset of microbubble vibration, *Ultrasound Med. Biol.* 33 (2007) 941-949.
- [11] N. De Jong, M.C. Emmer, T. Chin, A. Bouakaz, F. Mastik, D. Lohse, Compression-only behavior of phospholipid-coated contrast bubbles, *Ultrasound Med. Biol.* 33 (2007) 653-656.
- [12] J. Tu, J. Guan, Y. Qiu, T.J. Matula, Estimating the shell parameters of SonoVue® microbubbles using light scattering, *J. Acoust. Soc. Am.* 12 (2009) 2954-2962.
- [13] A.A. Doinikov, J.F. Haac, P.A. Dayton, Modeling of nonlinear viscous stress in encapsulating shells of lipid-coated contrast agent microbubbles, *Ultrasonics* 49 (2009) 269-275.
- [14] S. Paul, R. Nahire, S. Mallik, K. Sarkar, Encapsulated microbubbles and echogenic liposomes for contrast ultrasound imaging and targeted drug delivery, *Comput. Mech.* 53 (2014) 413-435.
- [15] S. Paul, A. Katiyar, K. Sarkar, K.D. Chatterjee, W.T. Shi, F. Forsberg, Material characterization of the encapsulation of an ultrasound contrast microbubble and its subharmonic response: Strain-softening interfacial elasticity model, *J. Acoust. Soc. Am.* 127 (2010) 3846-3857.
- [16] M. Overvelde, V. Garbin, J. Sijl, B. Dollet, N. De

- Jong, D. Lohse, M. Versluis, Nonlinear shell behavior of phospholipid-coated microbubbles, *Ultrasound Med. Biol.* 36 (2010) 2080-2092.
- [17] B. Helfield, X. Chen, B. Qin, F.S. Villanueva, Individual lipid encapsulated microbubble radial oscillations: Effects of fluid viscosity, *J. Acoust. Soc. Am.* 139 (2016) 204-214.
- [18] F. Forsberg, W.T. Shi, B.B. Goldberg, Subharmonic imaging of contrast agents, *Ultrasonics*, 38 (2000) 93-98.
- [19] F. Forsberg, J.B. Liu, W.T. Shi, J. Furuse, M. Shimizu, B. Barry, In vivo pressure estimation using subharmonic contrast microbubble signals: Proof of concept, *IEEE T. Ultrason. Ferr.* 52 (2005) 581-583.
- [20] P.M. Shankar, P.D. Krishna, V.L. Newhouse, Advantages of subharmonic over second harmonic backscatter for contrast-to-tissue echo enhancement, *Ultrasound Med. Biol.* 24 (1998) 395-399.
- [21] D. Adam, M. Sapunar, E. Burla, On the relationship between encapsulated ultrasound contrast agent and pressure, *Ultrasound Med. Biol.* 31 (2005) 673-686.
- [22] K.S. Andersen, J.A. Jørgen, Impact of acoustic pressure on ambient pressure estimation using ultrasound contrast agent, *Ultrasonics*, 50 (2010) 294-299.
- [23] A. Katiyar, K. Sarkar, F. Forsberg, Modeling subharmonic response from contrast microbubbles as a function of ambient static pressure, *J. Acoust. Soc. Am.* 129 (2011) 2325-2335.
- [24] L.M. Leodore, F. Forsberg, W.T. Shi, P5B-6 *in-vitro* pressure estimation obtained from subharmonic contrast microbubble signals, *Proc. IEEE Ultrason. Symp. (IUS)* (2007) 2207-2210.
- [25] W.T. Shi, F. Forsberg, J.S. Raichlen, L. Needleman B.B. Goldberg, Pressure dependence of subharmonic signals from contrast microbubbles, *Ultrasound Med. Biol.* 25 (1999) 275-283.
- [26] N. Mobadersany, A. Katiyar, K. Sarkar, Effects of ambient pressure on the subharmonic response from encapsulated microbubbles, *arXiv preprint arXiv: 1507.04829* (2015).
- [27] D. Chatterjee, P. Jain, K. Sarkar, Ultrasound-mediated destruction of contrast microbubbles used for medical imaging and drug delivery, *Phys. Fluids*, 17 (2005) 100603.
- [28] A. Katiyar, K. Sarkar, Excitation threshold for subharmonic generation from contrast microbubbles, *J. Acoust. Soc. Am.* 130 (2011) 3137-3147.
- [29] A. Katiyar, K. Sarkar, F. Forsberg, Modeling subharmonic response from contrast microbubbles as a function of ambient static pressure, *J. Acoust. Soc. Am.* 129 (2011) 2325-2335.
- [30] A.Y. Ammi, R.O. Cleveland, J. Mamou, G.I. Wang, S.L. Bridal, W.D. O'Brien, Ultrasonic contrast agent shell rupture detected by inertial cavitation and rebound signals, *IEEE T. Ultrason. Ferr.* 53 (2006) 126-136.
- [31] J.E. Chomas, P. Dayton, J. Allen, K. Morgan, K.W. Ferrara, Mechanisms of contrast agent destruction, *IEEE T. Ultrason. Ferr.* 48 (2001) 232-248.